Rock and Soil Mechanics

Volume 42 | Issue 1 Article 1

5-26-2021

Effect of normal stress on cyclic simple-shear behavior of gravel-structure interface

Da-kuo FENG
China Construction Seventh Engineering Division Corp. Ltd., Zhengzhou, Henan 450004, China

Jian-min ZHANG
Institute of Geotechnical Engineering, Tsinghua University, Beijing 100084, China,
zhangjm@tsinghua.edu.cn

Custom Citation

FENG Da-kuo, ZHANG Jian-min, . Effect of normal stress on cyclic simple-shear behavior of gravel-structure interface[J]. Rock and Soil Mechanics, 2021, 42(1): 18-26.

Rock and Soil Mechanics 2021 42(1): 18−26 ISSN 1000−7598
https: //doi.org/10.16285/j.rsm.2020.5656 rocksoilmech.researchcommons.org/journal

Effect of normal stress on cyclic simple-shear behavior of gravel-structure interface

FENG Da-kuo[1, 2], ZHANG Jian-min[1, 3]

1. State Key Laboratory of Hydroscience and Engineering, Tsinghua University, Beijing 100084, China
2. China Construction Seventh Engineering Division Corp. Ltd., Zhengzhou, Henan 450004, China
3. Institute of Geotechnical Engineering, Tsinghua University, Beijing 100084, China

Abstract: The cyclic simple-shear behavior of soil-structure interfaces under different normal stresses is of great significance in theoretical analysis and engineering practices. A series of interface tests between gravel and steel was conducted under different normal stresses using a 3D large-scale simple-shear apparatus, and the influence of normal stress on the cyclic simple-shear behavior of the interface was explored in detail. The normal stress plays a crucial role in the magnitudes of the shear behavior of the interface, including deforming and sliding displacements, shear stress, reversible and irreversible normal displacement, and cyclic shear strength, while it has slight influence on the relationship pattern of shear behavior. Increased normal stress leads to increased deforming displacement at the first few shear cycles, accelerated reduction and decreased stabilized amplitude of deforming displacement. Enhanced normal stress also results in increased shear modulus, decreased shear modulus coefficient at the first a few shear cycles, increased stabilized shear stress and cyclic shear strength of the interface. In addition, larger normal stress results in larger irreversible normal displacement, smaller peak reversible normal displacement, smaller transition tangential displacement and transition stress ratio of the interface. The cyclic shear strength behaves well in accordance with Mohr-Coulomb criteria, regardless of normal stress. Perfect consistency exists in the stress ratio versus tangential displacement response and irreversible normal displacement versus shear work density response, independent of normal stress, and can be described using hyperbolic models. These consistency characteristics will significantly simplify the constitutive modelling of soil-structure interfaces.

Keywords: soil−structure interface; cyclic simple-shear behavior; normal stress; consistency characteristics; strength anisotropy

1 Introduction

The soil−structure interface, which is composed of the structure plane and the soil adjacent to and constrained by the structure, exists widely in engineering practices, such as concrete-faced rockfill dam, buried piles and high-speed railways. Its behavior is different from the soil itself due to the strong constraint of the structure. The interface is the key medium for the stress and deformation transfer between the soil and structure, and therefore, plays a vital role in the stability of soil−structure system. A large number of researchers and engineers explored the monotonic and cyclic shear behavior of the interface and its influencing factors using direct-shear device, simple-shear device, ring torsional shear device and so on. The direct-shear test device is the most popular device for the interface testing because of the easy modification and handy operation of the test device and convenient preparation of test specimen. In addition, the relative movement between the soil and structure is clear and can be easily measured for direct-shear tests. However, the deforming and sliding displacements of the interface cannot be separated in the direct-shear tests.

By contrast, the simple-shear tests for the interface is able of separating the deforming and sliding displacements from total tangential displacement. More and more researchers examined the behavior of the soil−structure interface using simple-shear test device. Uesugi et al.[1] earlier explored the two-dimensional (2D) behavior of the sand−structure interface by simple-shear tests, and was the first to divide the tangential displacement of the interface into the sliding displacement and the displacement caused by shear deformation of the soil. The monotonic and cyclic behaviors of the sand−structure interface[1−6], the clay−structure interface[3, 7−9], and the gravel−structure interface[10−15] was examined in detail and the influence of soil properties[1−2, 5, 10], roughness of structure surface[1−2], shear path[2,5,8,15] and test type[1,3,6−7] were also addressed based on simple-shear tests.

The shear stress, shear strength, and volumetric deformation of the soil−structure interface depends on the normal stress. Therefore, it is a key factor influencing the interface behavior, and is a basic element that the

Received: 20 May 2020 Revised: 30 September 2020
This work was supported by the National Natural Science Foundation of China (52079126) and the National Key Research and Development Program (2017YFC0703906).
First author: FENG Da-kuo, male, born in 1984, PhD, Senior engineer, research interests: soil-structure interaction, green construction, prefabricated construction. E-mail: tpada@qq.com
Corresponding author: ZHANG Jian-min, male, born in 1960, PhD, Professor, mainly engaged in teaching and research in geotechnical engineering. E-mail: zhangjm@tsinghua.edu.cn

interface constitutive model should include. Numerous simple-shear tests were conducted to investigate the influence of the normal stress on the monotonic and cyclic behavior of the soil−structure interface[1−3,5,7,9−13]. Uesugi et al.[1] and Desai et al.[3] discovered that the normal stress had slight effect on the monotonic and cyclic shear strength of the interface, while Fakharian[2] suggested that the increased normal stress resulted in decreased shear strength of the sand−structure interface. In addition, the normal stress was also confirmed to remarkably affect the shear strength[7, 10], initial shear stiffness[10], normal displacement[5, 7] and shear stress ratio[5] from simple-shear tests of the interface. However, majorities of the previous simple-shear interface tests focused on the shear stress−displacement response of the interface at different normal stresses and the influence on the monotonic shear strength, initial shear stiffness and normal displacement. Zhang et al.[16] developed a large-scale test apparatus, called 80-ton 3-D multifunction apparatus for soil−structure (3DMAS) interface, and explored the monotonic and cyclic behavior of the gravel−structure interface from three-dimensional (3D) simple-shear tests[14−15]. Special attempts were made to discuss the significance of the normal stress on the soil deformation, interface thickness and shear strength of the interface due to monotonic shearing[14], and the effect of the shear path on 3D cyclic simple-shear behavior of the interface, the shear stress−displacement response, volumetric deformation, and shear strength at the same normal stress of 400 kPa. Few data were reported on the effect of the normal stress on the simple-shear behavior of the gravel−structure interface.

In this research, a series of the simple-shear tests was performed on the interface between the gravel and steel plate using the 3DMAS to investigate the cyclic simple-shear interface behavior at different normal stresses. A brief description of the test device, soil container and test materials is first given. The effect of normal stress on the cyclic simple-shear behavior of the gravel−structure interface is then discussed in detail, including deforming and sliding displacements, shear stress−displacement hysteretic response, irreversible and reversible volumetric deformation, and shear strength. Several constitutive laws of the interface, such as the consistency of the irreversible normal displacement, the phase transition of the reversible normal displacement, the consistency of the stress ratio−displacement hysteretic response, and the anisotropy and evolution of shear strength, are discussed. The new observations and conclusions of the stress-controlled behavior of the interface are finally drawn to provide the data and basis for the establishment and validation of the interface model.

2 Test configurations

The tested interface was composed of dry gravelly soil and a steel plate, which were described in detail by Feng et al.[14−15]. The gravel has some angularities with the diameters ranging from 5 mm to 16 mm (i.e., D_{min}=5 mm, D_{max}=16 mm) with a mean diameter of 9 mm. The poorly-graded gravel with a uniform distribution (C_u=1.8, C_c=0.9) was tamped into the round simple-shear container in five layers to the required dry density of 1780 kg/m^3. An isotropic steel plate was used as the structure plate, and the surface was uniformly notched with standard shapes of repeating quadrangular pyramid frustums of 2 mm high. The surface roughness of the steel plate is 2 mm (i.e., R=2 mm) and was kept invariable throughout shearing. Therefore, the normalized roughness of the interface is R_n=0.222.

The cyclic simple-shear tests of the gravel−structure interface were performed using a large-scale apparatus called 3DMAS, which was developed for 2D and 3D interface tests with high accuracy. Details of the 3DMAS was provided by Zhang et al.[16]. The simple-shear soil container was used for simple-shear interface tests since the 3DMAS was designed with modularization conception. The steel plate lied on the gravel specimen (Fig. 1) to ensure that the measured normal stress is the stress directly acting on the interface. The relative displacements of the rings were obtained using image-processing technique recorded by two cameras. Details of the simple-shear container and the measurement of tangential displacements were given by Feng et al.[14−15].

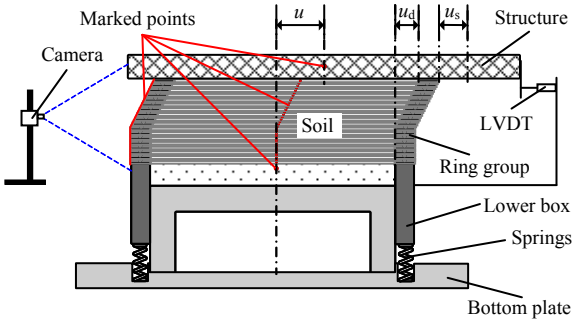

Fig. 1 Schematic view of simple-shear container for interface tests

3 Tangential deformation

Figure 2 shows the cyclic simple-shear behavior of the gravel−structure interface in two-way beeline shear path (total tangential displacement amplitude u_m=20 mm, normal stress σ=700 kPa). Three tangential displacements of the interface (illustrated in Fig. 1) and their amplitudes that will be reiterated to address the simple-shear behavior of the interface are defined as follows:

Total tangential displacement u[15]: referring to the tangential displacement of the structure plate relative to

the lower box of the simple-shear container.

Deforming displacement u_d [15]: defined as the tangential displacement induced by the shear deformation of the soil, and can be obtained from the total displacement of the ring group in the tangential direction.

Sliding displacement u_s [15]: defined as the displacement of the soil particles adjacent to the structure plate slipping relatively to the structure plate, and therefore, $u_s = u - u_d$.

Deforming displacement amplitude u_{dm}: half of the difference between the maximum and minimum deforming displacements at an individual shear cycle.

Sliding displacement amplitude u_{sm}: half of the difference between the maximum and minimum sliding displacements at an individual shear cycle.

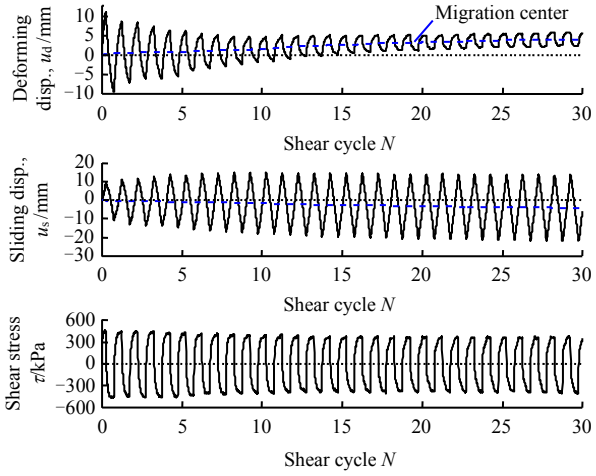

Fig. 2 Cyclic shear behavior of the interface (σ=700 kPa)

3.1 Deformation and sliding displacements

Distinct deforming and sliding displacements occur at the onset of shearing. The deforming displacement amplitude decreases and then tends to be stabilized with the increase in shear cycle, indicating that the gravel near the structure becomes stiffened due to cyclic shearing. By contrast, the sliding displacement amplitude increases due to cyclic shearing because of the maintenance of the total tangential displacement amplitude.

In addition, the deforming displacement migrates towards the positive direction (i.e., the initial shear direction), indicating the shear orientation effect, which refers to the orientation rearrangement of soil particles induced by initial shearing[15]. When the interface is initially sheared before the shear direction is reversed, the gravel particles rotate towards the initial shear direction due to restraint of structure plate, and produce plastic tangential deformation. This orientation rearrangement of the gravel particles would not be recovered inadequately when the shear direction is reversed, and would hinder the soil deformation towards the opposite direction, and therefore results in the migration of deforming displacement towards the initial shear direction. By contrast, the sliding displacement migrates towards the opposite direction in the view of the fact that the total tangential displacement amplitude remains invariable.

Figure 3 displays the cyclic histories of the deforming and sliding displacement amplitudes of the interface at different normal stresses (σ=200, 400, 700 and 1 000 kPa). It is demonstrated that the deforming displacement amplitude decreases gradually with cycling of total tangential displacement at different normal stresses. However, larger normal stress provides greater friction restraint of structure plate to the near gravel particles, and therefore results in larger deforming displacement at the first few shear cycles. On the other hand, increased normal stress would produce intensified crushing and rearrangement of the gravel particles near the structure plate, leading to accelerated soil compaction and stiffening due to cyclic shearing, and therefore lead to accelerated reduction in deforming displacement amplitude and decreased stabilized amplitude. When the normal stress is large (e.g., σ =700 and 1 000 kPa), the stabilized deforming displacement amplitude is almost the same, and is approximately smaller than $0.25D_{50}$. Correspondingly, larger normal stress results in smaller sliding displacement amplitude at the first few shear cycles, but faster increase in sliding displacement, and therefore brings about larger stabilized sliding displacement amplitude.

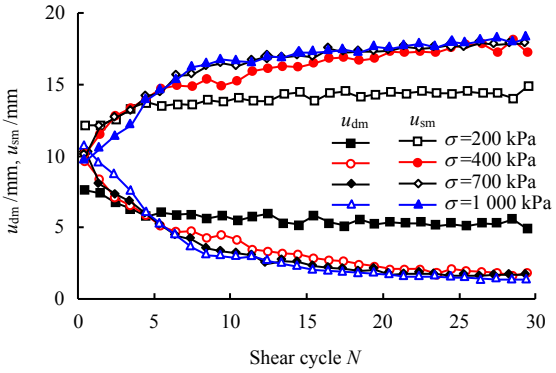

Fig. 3 Evolution of deforming and sliding displacement amplitudes of the interface at different normal stresses

Figures 4 and 5 provides the response of deforming and sliding displacement against total tangential displacement and the shear stress response against deforming and sliding displacements at selected shear cycles (i.e., N=1 and 10), further confirming the influence of normal stress on the deforming and sliding displacements. The deforming and sliding displacements grow gradually with the increase in total tangential displacement at different normal stresses. The growth rate of deforming displacement decreases and that of sliding displacement increases with the increase in total tangential displacement (Figs. 4(a), 4(b), 5(a) and 5(b)). At the first few shear

cycles (e.g., N=1), increased normal stress results in accelerated and slowed increase in deforming and sliding displacements, respectively, and hence leads to increased deforming displacement amplitude and decreased sliding displacement amplitude (Figs. 4(c) and 5(c)). When the interface is cyclically sheared to a certain extent (e.g., N=10), larger normal stress gives rise to slower and faster increase in deforming and sliding displacements, respectively, and therefore bring about smaller deforming displacement amplitude and larger sliding displacement amplitude (Figs. 4(d) and 5(d)).

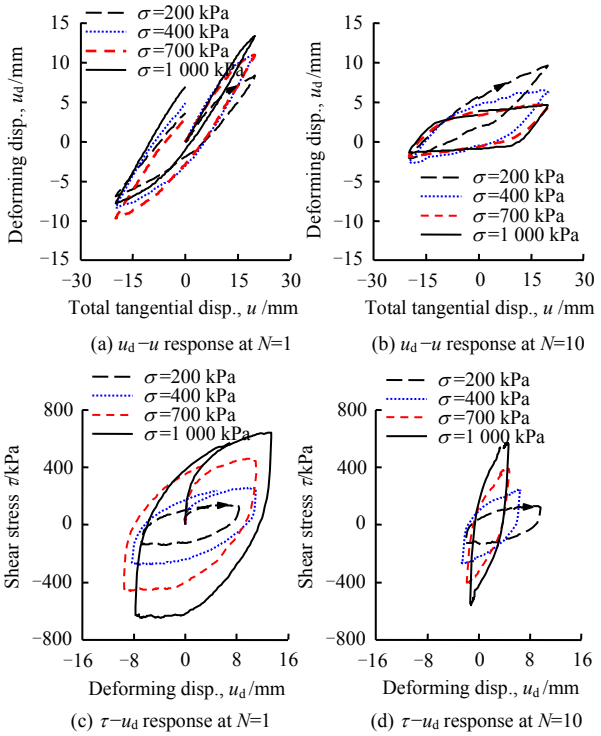

(a) u_d−u response at N=1 (b) u_d−u response at N=10

(c) τ−u_d response at N=1 (d) τ−u_d response at N=10

Fig. 4 Interface deforming displacement at different normal stresses

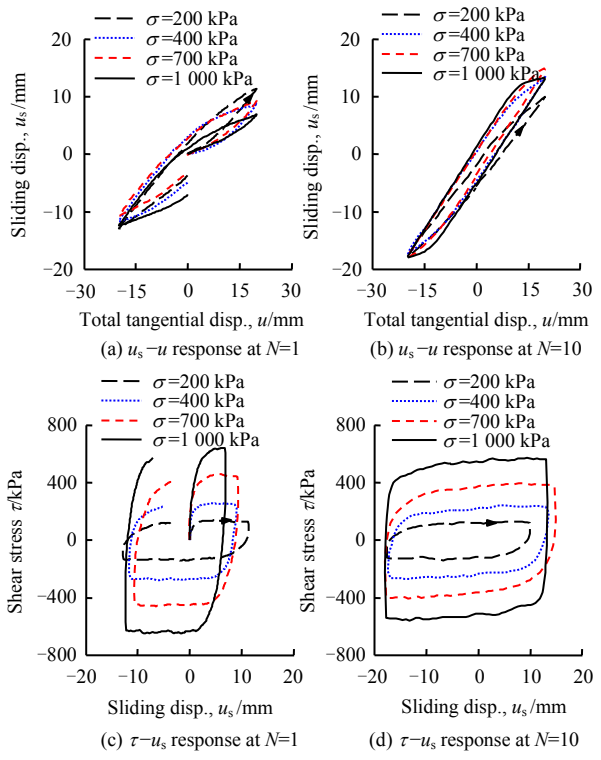

(a) u_s−u response at N=1 (b) u_s−u response at N=10

(c) τ−u_s response at N=1 (d) τ−u_s response at N=10

Fig. 5 Interface sliding displacement at different normal stresses

3.2 Shear stress−displacement hysteretic response

Figure 6 gives the hysteretic response of shear stress τ and stress ratio η against total tangential displacement u. The stress ratio is defined as the ratio of the shear stress to the corresponding normal stress (i.e., $\eta=\tau/\sigma$), and can eliminate the effect of normal stress and address the interface behavior at different normal stresses.

It is discovered from Figs. 4, 5 and 6 that the normal stress has slight influence on the relationship pattern of the interface behavior, but noticeably impacts on the magnitude. The shear stress and stress ratio grow gradually with deforming, sliding and total tangential displacements, and then tend to be stabilized, indicating that the strain-softening behavior is absent for the gravel−structure interface and that the hyperbolic model is suitable for the hysteretic response. However, the normal stress has significant influence on the shear stress, shear stiffness and shear stiffness coefficient. The shear stiffness refers to the slope of shear stress versus total tangential displacement hysteretic curves, and the shear stiffness coefficient is defined as the slope of stress ratio versus total tangential displacement curve. Increased normal stress gives rise to accelerated growth of shear stress and increased shear stiffness and shear stress. In addition, larger normal stiffness results in slower growth of stress ratio and smaller shear stiffness coefficient at the first few shear cycles (e.g., N=1). When the interface is cyclic sheared to a certain extent, larger normal stress leads to larger shear stiffness coefficient because of the more crushing and greater shear stiffening of the gravel particles near the structure plate.

Interestingly, the peak stress ratio is almost the same and the stress ratio versus total tangential displacement hysteretic curves are almost coincident except the initial shear stiffness coefficient at different normal stresses (Figs. 6(c) and 6(d)), indicating a perfect consistency of the stress ratio versus total tangential displacement hysteretic response, regardless of the normal stress. This consistency can be described by using the hyperbolic model and considering the initial shear stiffness coefficient, which will significantly simplify the constitutive description of the hysteretic response of the interface at different normal stresses. The curves of the stress ratio against deforming and sliding displacements are no longer coincident at different normal stresses, which is attributed to the different migrations and amplitudes, and therefore, the consistency behavior is absent.

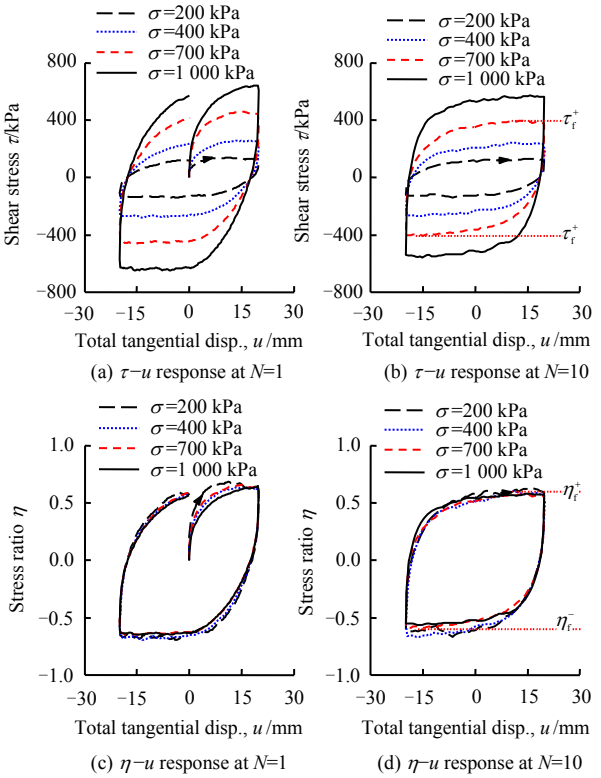

Fig. 6 Interface total tangential displacement at different normal stresses

4 Volumetric deformation

Figure 7 shows the cyclic histories of the normal displacement of the interface at different normal stresses. The contact area of the interface remains constant throughout shearing, and the normal displacement can therefore represent the volumetric deformation of the interface. Distinct normal displacement is caused by cyclic shearing, and can be divided into irreversible and reversible components[15]. The former is the maximum normal displacement at an individual shear cycle, and displays the general trend of volumetric deformation of the interface. The latter refers to the regular fluctuation of the normal displacement at an individual shear cycle, and can represent the recoverable volumetric deformation of the interface.

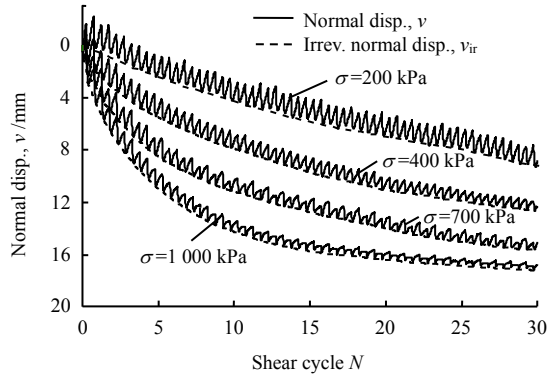

Fig. 7 Cyclic normal displacement of the interface against shear cycle at different normal stresses

4.1 Irreversible normal displacement

Figure 7 shows that irreversible normal displacement accumulates gradually and the accumulation is slowed due to cyclic shearing. The normal stress affects the magnitude and accumulation rate of the irreversible normal displacement. Increased normal stress results in intensified rearrangement and crushing of the gravel particles near the structure plate, and therefore leads to accelerated accumulation of the irreversible normal displacement at the first few shear cycles. When the interface is cyclically sheared to a certain extent, larger normal stress gives rise to smaller amount to be crushed and smaller crushing potential of the gravel particles because of the larger amount of the crushed gravel particles, and brings about slowed accumulation of the irreversible normal displacement. Moreover, increased normal stress results in larger irreversible normal displacement due to intensified rearrangement and crushing of the gravel particles.

It is demonstrated that the volumetric deformation of the interface is primarily caused by shearing. The shear work density[17] is introduced to quantify the shearing effect and shearing history of the interface, and is defined as the integral of the scalar product between the shear stress vector $\boldsymbol{\tau}$ and total tangential displacement increment vector $\mathrm{d}\boldsymbol{u}$, that is,

$$\omega_{\mathrm{s}} = \int \boldsymbol{\tau} \cdot \mathrm{d}\boldsymbol{u} = \int \left(\tau_x \mathrm{d}u_x + \tau_y \mathrm{d}u_y \right) \tag{1}$$

The shear work density could be simplified as follows in two-way beeline cyclic shear path because the interface is only sheared in a single tangential direction (i.e., τ_x=u_x=0 or τ_y=u_y=0),

$$\omega_{\mathrm{s}} = \int \tau \mathrm{d}u \tag{2}$$

Therefore, the shear work density refers to the integral of the area of the shear stress−displacement hysteretic curves of the interface.

The irreversible normal displacement response against the shear work density at different normal stresses in Fig. 8 indicates their perfect consistency behavior, independent of normal stress, since the shear work density has reflected the effect of the normal stress through the shear stress. This consistency behavior can be described using the following hyperbolic model:

$$v_{\mathrm{ir}} = \frac{\omega_{\mathrm{s}}}{B + A\omega_{\mathrm{s}}} \tag{3}$$

where the parameters A and B are the reciprocals of the ultimate magnitude and the initial accumulation rate of the irreversible normal displacement, respectively. Figure 8 demonstrates that the simulation results match with the test results well, and that Eq. (3) provides a unified description for the irreversible normal displacement. This consistency behavior and unified description will significantly simplify the constitutive modeling for the

irreversible normal displacement of the interface. In addition, the consistency behavior indicates an ultimate irreversible normal displacement, which depends on the material properties of the interface, regardless of the normal stress. Therefore, if the shear work density is ultimate, the irreversible normal displacement will approach the ultimate, where the gravel particles near the structure plate will be no more crushed.

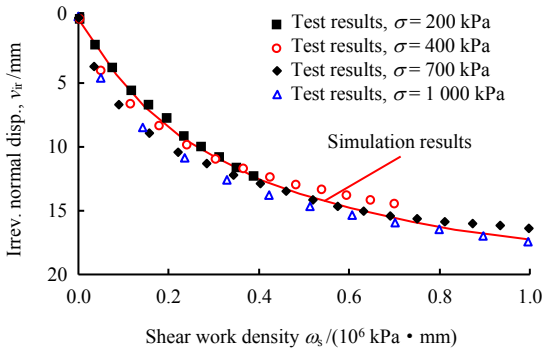

Fig. 8 Consistency of the irreversible normal displacement of the interface against shear work density at different normal stresses

4.2 Reversible normal displacement

Figure 9 presents the reversible normal displacement response v_{re} against the total tangential displacement u and the stress ratio η at the selected shear cycle (i.e., N=10). The reversible normal displacement response against deforming and sliding displacements and shear stress exhibit similar behavior, and therefore are omitted for brevity.

The reversible normal displacement grows gradually with continuing shearing, and achieves its peak $v_{re,p}$ at the limiting total tangential displacement and at the peak stress ratio. The reversible normal displacement will recover when the shear direction is reversed and the interface is unloaded. The normal stress primarily influences the peak reversible normal displacement and its phase transition, which refers to the characteristics that the magnitude of the reversible normal displacement starts increasing from decreasing and that the interface starts dilatancy from compression. The critical point that the magnitude of the reversible normal displacement stop decreasing and starts increasing is considered as the transition point, and the corresponding shear stress and stress ratio is referred to as the transition shear stress (denoted as τ_t) and transition stress ratio (denoted as η_t), respectively. The total tangential displacement for the magnitude of the reversible normal displacement to stop decreasing is defined as the transition tangential displacement u_t. These defined parameters (i.e., τ_t, η_t and u_t) are illustrated in Fig. 9 and quantify the conditions that the interface needs for dilatancy.

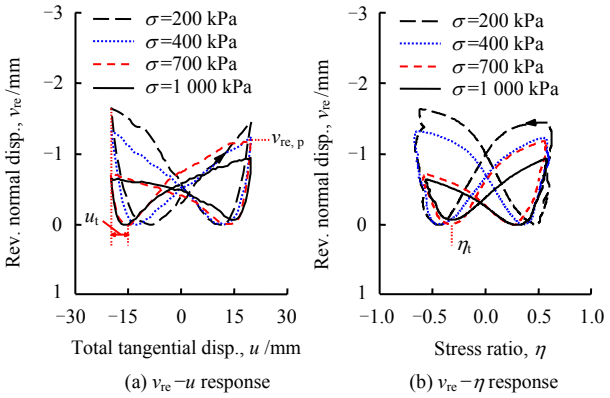

Fig. 9 Reversible normal displacement of the interface at different normal stresses and definitions of transition tangential displacement and transition stress ratio (N=10)

Figure 10 shows the peak reversible normal displacement of the interface $v_{re,p}$ against the normal stress σ at given shear cycles (N=1, 5, 10, 20 and 30). The peak reversible normal displacement decreases gradually and then tends to be stabilized as cyclic shearing continues at different normal stresses. The peak magnitude and its evolution of the reversible normal displacement are noticeably affected by the normal stress. Larger normal stress provides greater compression effect of the structure plate on the gravel particles, results in more constraints for the gravel particles to climb and roll, and therefore leads to smaller peak reversible normal displacement if exists. In addition, increased normal stress brings about intensified crushing of the gravel particles near the structure plate subjected to cyclic shearing, and therefore gives rise to decreased stabilized value of the peak reversible normal displacement and reduced shear cycles for the peak reversible normal displacement to be stabilized. Therefore, the peak reversible normal displacement depends on the development of the reversible normal displacement and the crushing amount of the gravel particles near the structure plate. When the normal stress is small (e.g., σ=200 kPa), the gravel particles near the structure plate are crushed less, and the peak reversible normal displacement tends to be stabilized after the 5th shear cycle (i.e., $N\geqslant5$) and the stabilized value is relatively large. When the normal stress is relatively large (e.g., σ=1 000 kPa), the peak reversible normal displacement is not completely stabilized at the 20th shear cycle (i.e., N=20), and the stabilized value is relatively small.

Figure 11 gives the cyclic histories of the transition tangential displacement u_t and transition stress ratio η_t of the interface against shear cycle at different normal stresses. The transition tangential displacement presents similar magnitude subjected to the initial shearing (i.e., N=1) at different normal stresses. Larger normal stress leads to faster reduction and smaller magnitude of the transition tangential displacement. This is attributed to more crushing and smaller mean diameters of the gravel

particles near the structure plate, and therefore smaller tangential displacement for the interface to dilate.

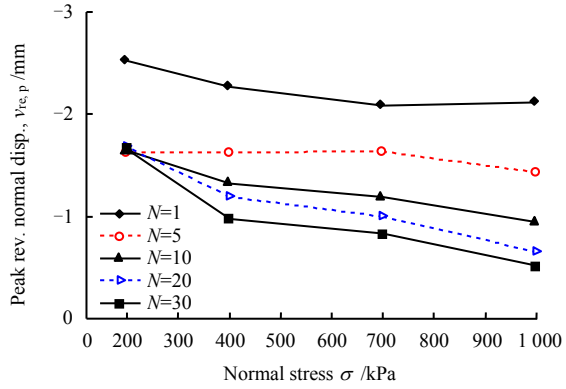

Fig. 10 Relationship of peak reversible normal displacement against normal stress

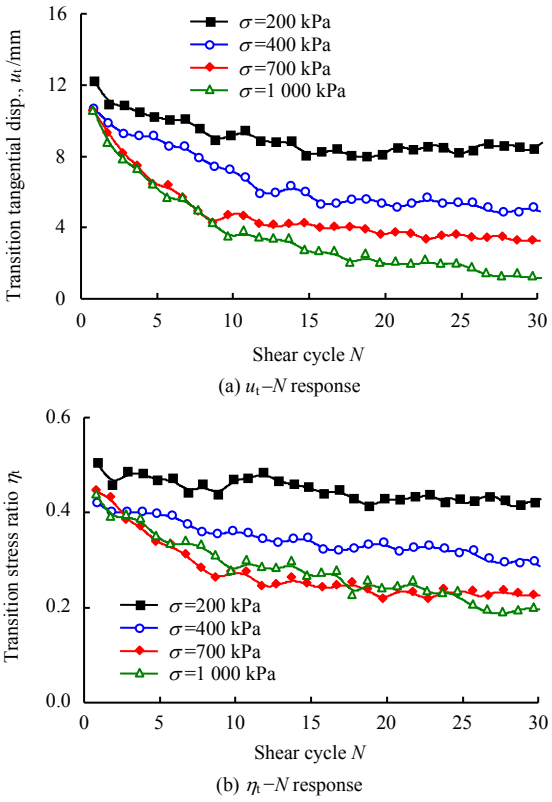

Fig. 11 Cyclic behavior of transition tangential displacement and transition stress ratio of the interface against shear cycle at different normal stresses

The transition stress ratio and transition shear stress exhibit similar response to the transition tangential displacement. However, increased normal stress leads to increased transition shear stress, though the transition shear stress presents similar changing trend to the transition stress ratio. This finding can also be confirmed by the transition shear stress response against the normal stress in Fig. 12. In addition, the transition shear stress presents a linear relationship with the corresponding normal stress at the initial shearing. This line is considered to be the transition line, which lies below the shear strength line. The transition shear stress decreases gradually as cyclic shearing continues, and the relationship curve between the transition shear stress and the normal stress is no longer linear, and gradually gets away from the shear strength line.

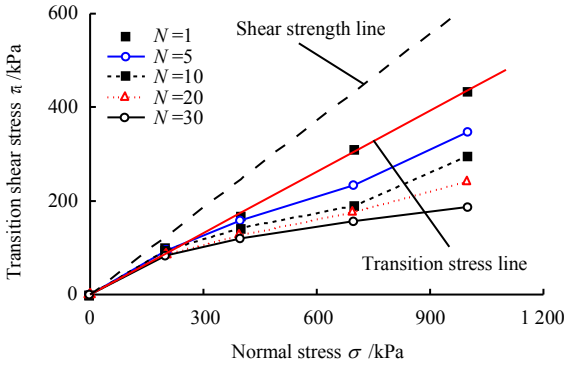

Fig. 12 Relationship of transition shear stress of the interface against normal stress

5 Shear strength

Figure 6 reveals that the shear stress grows gradually and then tends to stabilize at the peak value under shearing in the positive direction. The shear stress diminishes rapidly at the reversal of the shear direction, again grows gradually and then tends to stabilize at another peak value with the shearing in the negative direction. The peak shear stresses mobilized in the positive direction (i.e., the initial shear direction) and the negative direction are considered as the cyclic shear strength in the positive and negative directions[15] (denoted as τ_f^+ and τ_f^- illustrated in Fig. 6(b)), respectively, and the corresponding peak stress ratios are the cyclic strength index in the positive and negative directions (denoted as η_f^+ and η_f^- illustrated in Fig. 6(d)), respectively.

It is demonstrated that the cyclic shear strength of the interface is mobilized twice, respectively in the positive and negative directions at an individual shear cycle. Interestingly, the shear strength mobilized in the positive direction τ_f^+ is not the same, but is smaller than that mobilized in the negative direction τ_f^-, indicating an obvious anisotropy in the shear strength due to simple-shearing, which also occurs in other cyclic shear paths (e.g., two-way cross, and one-way and two-way circular shear paths)[15]. This strength anisotropy of the interface is also caused by the shear orientation effect, and is the macroscopic reflection and response of the microscopic anisotropy of the gravel particles near the structure plate caused by the initial shearing. The interface requires more shear stress to overcome the orientation rearrangement of the gravel particles and the shear orientation effect when it is sheared in the negative direction, and therefore the cyclic shear strength is larger than that in the positive direction. This strength anisotropy can also be confirmed by the cyclic histories of the shear strength against shear cycle in Fig. 13.

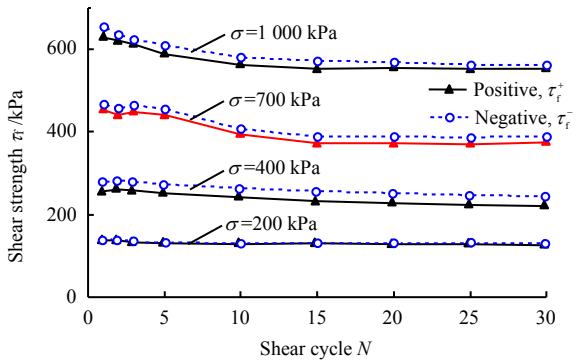

Fig. 13 Cyclic shear strength of the interface against shear cycle at different normal stresses

The anisotropy extent of shear strength $\Delta\tau_f$ is introduced herein to quantify the strength anisotropy, and is defined as the difference of the shear strengths of the interface in the negative and positive directions (i.e., $\Delta\tau_f=\tau_f^- - \tau_f^+$). The anisotropy extent of strength index ($\Delta\eta_f$) is defined as the difference of the strength index of the interface in the negative and positive directions (i.e., $\Delta\eta_f=\eta_f^- - \eta_f^+$), and can be obtained from the ratio of the anisotropy extent of shear strength to the corresponding normal stress under constant normal load condition (i.e., $\Delta\eta_f = \Delta\tau_f / \sigma$). The anisotropy extents of shear strength and strength index at different normal stresses in Fig. 14 reveal that they reach the smallest at the normal stress of 200 kPa (i.e., σ=200 kPa), and increase to the largest at the normal stress of 400 kPa (i.e., σ=400 kPa), followed by a distinct reduction. When the normal stress is small, the shear orientation effect is weak due to the low friction restraint of the structure plate to the nearby gravel particles, and therefore the anisotropy extent of shear strength and strength index are small. The friction restraint of the structure plate to the nearby gravel particles increases with the increase in the normal stress, the anisotropy extent of shear strength and strength index are magnified because of the intensified shear orientation effect. When the normal stress increases to a certain extent, the compression effect of the structure plate to the nearby gravel particles is dominate over the friction restraint. Increased normal stress results in intensified compression effect and difficulties in the climbing and rolling of the gravel particles, and therefore leads to minified anisotropy extent of shear strength and strength index.

Figure 13 shows that the shear strength of the interface decreases gradually and then tends to be stabilized as cyclic shearing continues, which can also be found in Fig. 6. This phenomenon indicates distinct evolution characteristics of the shear strength due to cyclic shearing[15], which also applies to the strength index under constant normal load condition. The evolution of the shear strength and the strength index directly gives rise to the gradual reduction of the anisotropy extent of strength index, which can be confirmed in Fig. 14. The shear strength response of the interface against normal stress at given shear cycles (N=1, 10 and 30) in Fig. 15 displays that the cyclic shear strengths of the interface in the positive and negative directions both present a linear relationship with the normal stress, and both can be expressed using the Mohr-Coulomb failure criteria ($\tau_f=\sigma\tan\varphi_i$), which is similar to the monotonic shear strength[15]. However, the friction angles of the interface φ_i are different in the positive and negative direction because of the strength anisotropy, and decrease gradually with cyclic shearing attributed to the evolution characteristics. The friction angles of the interface are 32.2° and 33.6° at 1st shear cycle, 29.6° and 30.5° at 10th shear cycle, and 28.7° and 29.9° at 30th shear cycle, in the positive and negative direction, respectively.

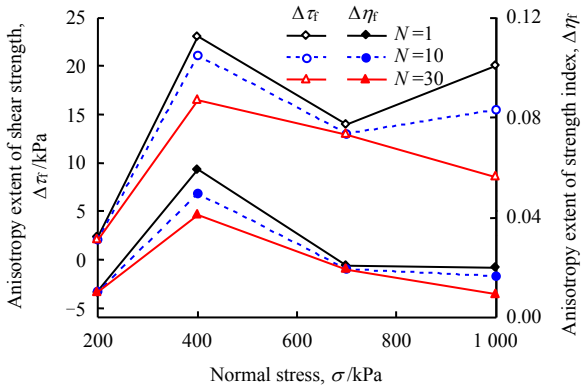

Fig. 14 Relationship of the anisotropy extent of the shear strength of the interface against normal stress

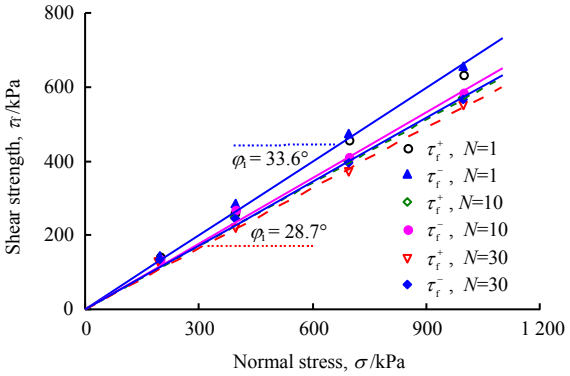

Fig. 15 Relationships of the shear strength of the interface against normal stress

6 Conclusions

A series of simple-shear interface tests was conducted using the 3DMAS to explore the cyclic simple-shear behavior of the gravel−structure interface at different normal stresses. The effects of the normal stress on the cyclic simple-shear behavior of the interface, including tangential deformation, volumetric deformation and shear strength, were addressed in detail. The new observations and conclusions of the cyclic simple-shear behavior of the interface are summarized as follows.

(1) Distinct deforming and sliding displacements take place at the onset of shearing. Deforming displacement amplitude decreases gradually and migrates towards the initial shear direction as cyclic shearing continues, attributed to the shear stiffening effect and shear orientation

effect, respectively. Increased normal stress results in magnified deforming displacement amplitude at the first few shear cycles, and leads to accelerated reduction and decreased stabilized magnitude of the deforming displacement amplitude.

(2) The normal stress has significant influence on the shear stress and shear stiffness. Larger normal stress gives rise to larger shear stiffness and stabilized shear stress, but leads to smaller shear stiffness coefficient at the first few shear cycles. Perfect consistency exists in the stress ratio versus total tangential displacement hysteretic response, regardless of the normal stress. This consistency behavior can be well captured using the hyperbolic model considering initial shear stiffness coefficient, which will remarkably simplify the constitutive modeling of the hysteretic response of the interface.

(3) The irreversible normal displacement of the interface grows with the increase in normal stress. The irreversible normal displacement response against the shear work density presents good consistency behavior, regardless of the normal stress. The hyperbolic model can provide a unified description for this consistency behavior, which will noticeably simplify the constitutive modeling of the irreversible normal displacement of the interface. Ultimate irreversible normal displacement is found for the gravel−structure interface, which depends on the material properties of the interface, instead of the normal stress.

(4) The evolution and phase transition of the peak reversible normal displacement are greatly influenced by the normal stress. Increased normal stress results in decreased peak reversible normal displacement, and leads to magnified shear cycles for the reversible normal displacement to achieve stabilized value. The transition tangential displacement and transition stress ratio present similar magnitude subjected to the initial shearing (i.e., N=1) at different normal stresses, and both decrease gradually as cyclic shearing continues. Larger normal stress brings about smaller transition tangential displacement and transition stress ratio when the interface is cyclically sheared to a certain extent.

(5) The shear strength behaves well in accordance with the Mohr-Coulomb criteria from simple-shear tests. The cyclic shear strength in the positive direction is smaller than that in the negative direction, indicating distinct strength anisotropy attributed to the shear orientation effect. The anisotropy extent of shear strength increases with increasing normal stress, and achieves the peak at the normal stress of 400 kPa (i.e., σ=400 kPa), followed by an obvious reduction. Distinct evolution characteristics occur in the cyclic shear strength, strength index and their anisotropy extents, which decrease gradually and then tend to be stabilized as cyclic shearing continues.

References

[1] UESUGI M, KISHIDA H. Influential factors of friction between steel and dry sands[J]. Soils and Foundations, 1986, 26(2): 33−46.

[2] FAKHARIAN K. Three-dimensional monotonic and cyclic behavior of sand-steel interfaces: testing and modeling[D]. Ottawa: University of Ottawa, 1996.

[3] DESAI C S, RIGBY D B. Cyclic interface and joint shear device including pore pressure effects[J]. Journal of Geotechnical and Geoenvironmental Engineering, 1997, 123(6): 568−579.

[4] ZHANG Dong-ji, LU Ting-hao. Establishment and application of an interface model between soil and structure[J]. Chinese Journal of Geotechnical Engineering, 1998, 20(6): 62−66.

[5] OUMAROU T A, EVGIN E. Cyclic behaviour of a sand-steel plate interface[J]. Canadian Geotechnical Journal, 2005, 42(6): 1695−1704.

[6] VIEIRA C S, LOPES M D L, CALDEIRA L. Sand-nonwoven geotextile interface shear strength by direct shear and simple shear tests[J]. Geomechanics and Engineering, 2015, 9(5): 601−618.

[7] XU Ze-you, LU Ting-hao, DING Ming-wu. Shear properties at interface between highly plastic clay and concrete[J]. Journal of Hohai University (Natural Sciences), 2009, 37(1): 71−74.

[8] WANG Wei, LU Ting-hao, ZAI Jin-min, et al. Negative shear test on soil-concrete interface using simple shear apparatus[J]. Rock and Soil Mechanics, 2009, 30(5): 1303−1306.

[9] GAO Jun-he, YU Hai-xue, ZHAO Wei-bing. Characteristics study of interface between soil and concrete by using large size single shear apparatus and numerical analysis[J]. China Civil Engineering Journal, 2000, 33(4): 42−46.

[10] WU Jun-shuai, JIANG Pu. Dynamic shearing behavior of soil-concrete interface[J]. Chinese Journal of Geotechnical Engineering, 1992, 14(2): 61−66.

[11] ZHOU Xiao-wen, GONG Bi-wei, DING Hong-shun, et al. Large-scale simple shear test on mechanical properties of interface between concrete face and gravel underlayer[J]. Chinese Journal of Geotechnical Engineering, 2005, 27(8): 876−880.

[12] ZHANG Zhi-jun, RAO Xi-bao, WANG Zhi-jun, et al. Experimental study on influence of slurry thickness on mechanical behavior of interface between gravel and concrete[J]. Rock and Soil Mechanics, 2008, 29(9): 2433−2438.

[13] PENG Kai, ZHU Jun-gao, ZHANG Dan, et al. Study of mechanical behaviors of interface between coarse-grained soil and concrete by simple shear test[J]. Chinese Journal of Rock Mechanics and Engineering, 2010, 29(9): 1893−1900.

[14] FENG Da-kuo, ZHANG Jian-min. Monotonic and cyclic behaviors of coarse-grained soil-structure interface using large-scale simple shear device[J]. Chinese Journal of Geotechnical Engineering, 2012, 34(7): 1201−1208.

[15] FENG D K, ZHANG J M, DENG L J. Three-dimensional monotonic and cyclic behavior of a gravel-steel interface from large-scale simple-shear tests[J]. Canadian Geotechnical Journal, 2018, 55(11): 1657−1667.

[16] ZHANG Jian-min, HOU Wen-jun, ZHANG Ga, et al. Development of a 3D soil-structure interface test apparatus and its application[J]. Chinese Journal of Geotechnical Engineering, 2008, 30(6): 889−894.